REACTIVE POWER CONTROL WITH THREE-PHASE INVERTER FOR GRID-CONNECTED PHOTOVOLTAIC SYSTEM

ĐIỀU KHIỂN CÔNG SUẤT PHẢN KHÁNG BẰNG INVERTER BA PHA CHO HỆ THỐNG NGUỒN ĐIỆN MẶT TRỜI HÒA LƯỚI

Nguyen Quang Thuan[1,*], Nguyen Duc Tuyen[2], Do Van Long[2], Ninh Van Nam[1]

ABSTRACT

In recent years, renewable energy sources have greatly affected the structure and operation of power systems. Previously, grid-connected PV generators using inverters were only allowed to generate active power to ensure the utilities to adjust the voltage in the distribution grid. It is no longer optimal for system power transmission and system stability, especially when solar power sources with a capacity of hundreds of MWs having a role in regulating grid voltage. Accordingly, this paper proposes a smart inverter model of a grid-connected PV system that can regulate the reactive power. We use PSCAD software to simulate and analyze the grid-connected solar PV system. Simulation results show the feasibility of this control model.

Keywords: *Photovoltaic; reactive power control; grid-connected Inverter; MPPT; Clarke and Park transformation.*

TÓM TẮT

Trong những năm gần đây, sự tham gia của các nguồn năng lượng tái tạo ảnh hưởng lớn đến cấu trúc và sự vận hành của hệ thống điện. Trước đây, các nguồn điện mặt trời phân tán khi hòa lưới được thiết lập chỉ phát công suất tác dụng. Hiện nay khi số lượng và công suất đặt của các nguồn năng lượng mặt trời ngày một tăng, khả năng điều khiển phát đồng thời công suất tác dụng và công suất phản kháng trở nên rất quan trọng cho vận hành hệ thống điện. Nhằm mục đích giải quyết vấn đề trên, bài báo này đề xuất một mô hình inverter của hệ thống điện mặt trời pin quang điện hòa lưới có khả năng điều chỉnh công suất phản kháng. Nghiên cứu sử dụng phần mềm PSCAD để mô phỏng và phân tích hệ thống điện mặt trời pin quang điện hòa lưới. Kết quả mô phỏng chỉ ra tính khả thi của mô hình điều khiển này.

Từ khóa: *Điện mặt trời; điều khiển công suất phản kháng; biến tần nối lưới; MPPT; biến đổi Clarke và Park.*

[1]Hanoi University of Industry
[2]School of Electrical Engineering, Hanoi University of Science and Technology
[*]Email: thuannq.haui@gmail.com
Received: 15/01/2020
Revised: 19/6/2020
Accepted: 26/02/2021

1. INTRODUCTION

The last decades, solar energy has grown rapidly worldwide due to the need for supplying the power demand. The most efficient technology to convert this energy into electricity is Photovoltaic (PV) technology [1]. Almost large current PV systems are connected to the grid because many advantages are reduction in the costs of the PV panels or capability to supply AC loads and inject active power, from the photovoltaic system to the grid, relieving the grid demand (distributed generation) [2]. All PV grid-connected systems are using three-phase inverters to utilize PV power sources. Previously, the PV grid-connected systems only supplied active power, but now the systems with PV inverters entirely possibly provided reactive power for the utility grid to improve power quality [3].

This paper presents the modelling method for maximum power point tracking (MPPT) controller. MPPT is a DC-DC converter that is used to ensure that the PV module always operates at the maximum power point. The MPPT method algorithm which this paper focuses on is perturbation and observation (P&O) method [4]. Along with that is the active and reactive power control with three-phase inverter using αβ and utilize transformation. This paper has references and development from previous studies in [1, 5, 6]. All of the modellings are designed in PSCAD/EMTDC environment. The simulation results indicate that this control method can perform accurate and feasible for the design of large PV systems.

2. PV GRID-CONNECTED CONDITIONING SYSTEM

Figure 1 shows a configuration of the three-phase PV grid-connected system. It consists of a PV array, a DC-DC boost converter, a DC-link capacitor, a DC-AC inverter, a harmonic reduction filter, a three-phase Δ/Y transformer.

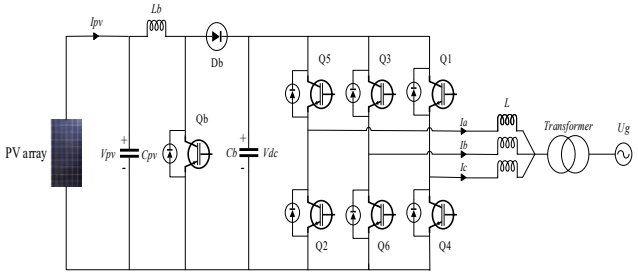

Figure 1. Configuration of three-phase PV grid-connected system

2.1. Solar Cell Model

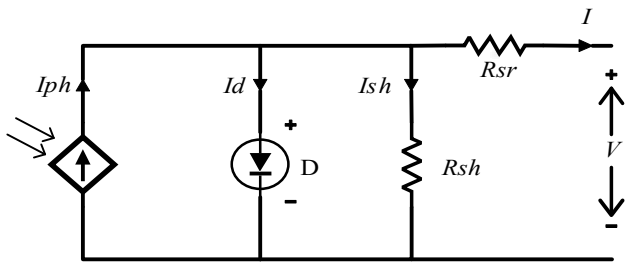

Figure 2. The equivalent circuit of the solar cell

Figure 2 is the equivalent circuit of the solar cell contains a photovoltaic current source anti-parallel with diode, shunt resistance, and series resistance [7].

Kirchhoff's current law provides:

$$I = I_{ph} - I_d - I_{sh} \quad (1)$$

Thus, the relationship between the output current-voltage is expressed by the following equation:

$$I = I_{ph} - I_0\left[\exp\left(\frac{V+IR_{sr}}{nkT_c/q}\right)-1\right]-\frac{V+IR_{sr}}{R_{sh}} \quad (2)$$

Where I is the PV output current, V is the PV output voltage, I_{ph} is the photovoltaic current, I_0 is the saturation current, R_{sr} is the series resistance, R_{sh} is the shunt resistance, q is the electron charge, n is the diode ideality factor, K is the Boltzmann constant, T_c is the cell temperature.

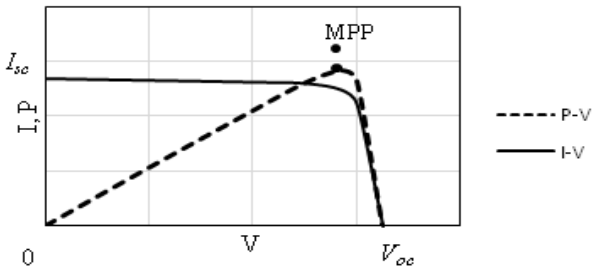

Figure 3. P-V and I-V characteristics of PV cell

Figure 3 shows the typical output characteristics and the maximum power point of PV cell where MPP is a maximum power point, V_{oc} is open-circuit voltage, I_{sc} is short circuit voltage

2.2. The DC-DC boost converter

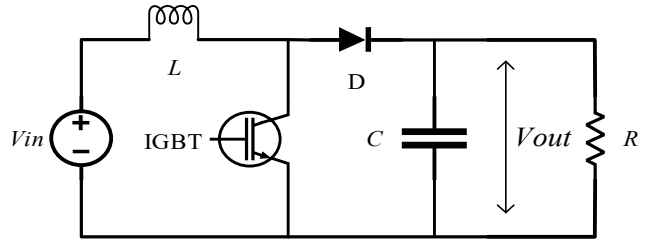

Figure 4. The equivalent circuit of the DC-DC Boost Converter

The DC-DC boost converter increases the output voltage of the PV array from the low level of input voltage to a high level of the output voltage. The boost converter mainly consists of resistance, inductor, diode, and capacitor operate in two modes. During the first mode when the switch is closed, the current rises through diode and inductor. During this interval, diode D is off. During the second mode, when the switch is opened the current flow through inductor, capacitor, diode, and load [8]. Figure 4 shows the equivalent circuit of the DC-DC Boost Converter.

$$D = 1 - \frac{V_{in}}{V_{out}}$$ where D is Duty Ratio

DC-DC switching is regulated by using different MPPT algorithms and techniques. The MPPT algorithms will be modelling in the next section.

2.3. The Perturb and Observe (P&O) MPPT algorithm

The MPPT takes the input of voltage and current from the PV source output and sets the DC link voltage reference at the inverter input side. As a result, when the DC link voltage maintains the reference value, the PV source can inject the maximum available power at specific irradiation and temperature [9]. As soon as the inverter output current matches the MPPT current due to the set point of MPPT voltage, the inverter settles at the operating point of maximum power output [1].

There are many MPPT algorithms have been published over the past decades. The three algorithms that are most appropriate for PV grid-connected systems are Perturb and Observe (P&O), incremental conductance (IC), and fuzzy logic control (FLC). In this subsection, we focus on describing the P&O algorithm [4].

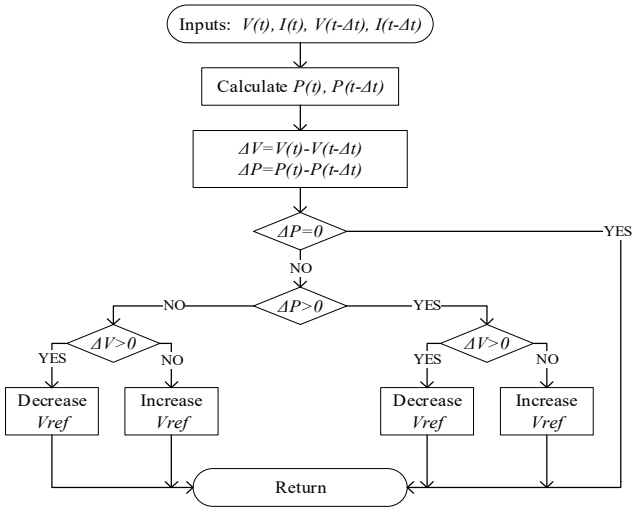

Figure 5. The flowchart of the P&O algorithm

In this method, based on comparing the actual value of the power with the previous value, the next perturbation is decided. If the power increases, the perturbation should continue to keep the same direction, and if the power decreases, we have an overrun of the MPP so the next perturbation should be in the opposite direction. The process is repeated until the MPP is reached. Because the method only compares the PV power, implementation is simple. The flowchart of the P&O algorithm is shown in Figure 5 [10].

2.4. Active and Reactive Power Control

To implement active power (P) and reactive power (Q) control, the quantities such as current and voltage are transferred from the stationary reference frame to the synchronous reference frame via Clarke and Park Transformation [11].

The following matrices are The Clarke Transformation and The Inverse Clarke Transformation, respectively. The V_o component does not exist in a balanced symmetrical condition.

$$\begin{bmatrix} V_\alpha \\ V_\beta \\ V_0 \end{bmatrix} = \frac{2}{3}\begin{bmatrix} 1 & -\frac{1}{2} & -\frac{1}{2} \\ 0 & \frac{\sqrt{3}}{2} & -\frac{\sqrt{3}}{2} \\ \frac{1}{2} & \frac{1}{2} & \frac{1}{2} \end{bmatrix}\begin{bmatrix} V_a \\ V_b \\ V_c \end{bmatrix} \quad \begin{bmatrix} V_a \\ V_b \\ V_c \end{bmatrix} = \begin{bmatrix} 1 & 0 & 1 \\ -\frac{1}{2} & \frac{\sqrt{3}}{2} & 1 \\ -\frac{1}{2} & -\frac{\sqrt{3}}{2} & 1 \end{bmatrix}\begin{bmatrix} V_\alpha \\ V_\beta \\ V_0 \end{bmatrix} \quad (3)$$

The following matrices are the Park Transformation and the Inverse Park Transformation, respectively.

$$\begin{bmatrix} V_d \\ V_q \\ V_0 \end{bmatrix} = \begin{bmatrix} \cos\theta & \sin\theta & 0 \\ -\sin\theta & \cos\theta & 0 \\ 0 & 0 & 1 \end{bmatrix}\begin{bmatrix} V_\alpha \\ V_\beta \\ V_0 \end{bmatrix} \quad \begin{bmatrix} V_\alpha \\ V_\beta \\ V_0 \end{bmatrix} = \begin{bmatrix} \cos\theta & -\sin\theta & 0 \\ \sin\theta & \cos\theta & 0 \\ 0 & 0 & 1 \end{bmatrix}\begin{bmatrix} V_d \\ V_q \\ V_0 \end{bmatrix} \quad (4)$$

The active and reactive power are:

$$P = V_d I_d + V_q I_q;\ Q = V_q I_d - V_d I_q \quad (5)$$

The V_q equal to zero when the synchronous reference frame is synchronized with the grid voltage [12]. Therefore, the power equations reduce to

$$P = V_d I_d;\ Q = -V_d I_q \quad (6)$$

To convey entire maximum PV power to the grid, the reference currents can be computed as:

$$I_{d\_ref} = \frac{P_{ref}}{V_d} = \frac{P_{pv}}{V_d} = \frac{P_{max}}{V_d};\ I_{q\_ref} = \frac{Q_{ref}}{V_d} \quad (7)$$

In Figure 7, the voltage output of the inverter can be founded as:

$$\frac{d\vec{i}}{dt} = \frac{\vec{V} - \vec{V}_{grid}}{L} \quad (8)$$

$$\frac{d}{dt}\begin{bmatrix} I_d \\ I_q \end{bmatrix} = \begin{bmatrix} 0 & -\omega \\ \omega & 1 \end{bmatrix}\begin{bmatrix} I_d \\ I_q \end{bmatrix} + \begin{bmatrix} 1/L & 0 \\ 0 & 1/L \end{bmatrix}\begin{bmatrix} V_d - V_{d\_grid} \\ V_q - V_{q\_grid} \end{bmatrix} \quad (9)$$

The equivalent equations are:

$$V_d = V_{d\_grid} - \omega L I_q;\ V_q = V_{q\_grid} + \omega L I_d \quad (10)$$

Therefore the reference voltages are:

$$V_{d\_ref} = V_{d\_feedback} + V_{d\_grid} - \omega L I_q \quad (11)$$

$$V_{q\_ref} = V_{q\_feedback} + \omega L I_d \quad (12)$$

The reference voltages (in three-phase) is then compared with the triangular waveform at a constant frequency to control the switches ON or OFF of inverter.

The proposed control schemes are shown in Figure 7. In this Figure, the Phase Locked Loop (PLL) keeps the reference input signal with output signal synchronized in frequency and phase. The most basic PLL structure consists of a phase detector block for generating a phase error signal between the input and the output signal of the PLL [13]. Figures 6 is a schematic block diagram of the PLL. The K_p and K_i are chosen in this model are 0.16 and 2.51, respectively. The PI controller of current control is designed in the same manner with the PLL with the K_p and K_i for active power control 0.5; 0.2, respectively. And the K_p and K_i for reactive power control 0.3; 0.02, respectively.

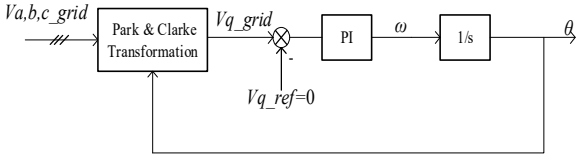

Figure 6. Schematic block diagram of the PLL

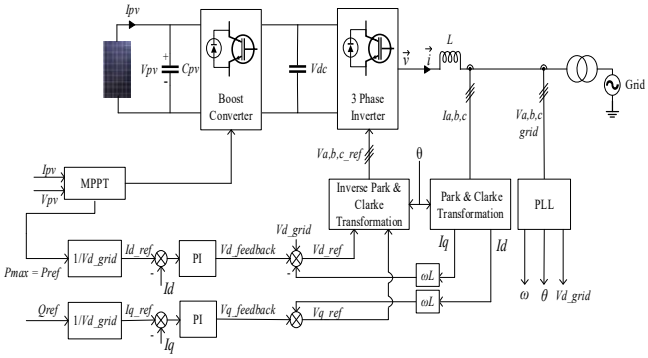

Figure 7. Proposed control scheme

3. SIMULATION RESULTS

In the simulation model, 22x250 numbers of series-parallel combinations of solar modules are connected, and the results are illustrated for the solar irradiance 1000W/m^2 at 25°C. All the parameters of the system are indicated in Table 1.

Table 1. The parameters of the PV system simulation

The parameters of system	
Temperature	25°C
Irradiance	1000W/m^2
Grid voltage (Line to line, RMS)	35kV
Frequency of PV system	50Hz
Inductance of passive filter	L = 125.10^{-6}H
DC link capacitor	C = 1950.10^{-6}F
Switching frequency of IGBT	8kHz
Transformer Δ/Y-0.6/35kV	560kVA

The output voltage and current of the PV array can be seen in Figure 8. Then, Figure 9 shows the output DC voltage and DC current of the DC-DC boost converter.

The PV power, according to the calculation, is 0.3MW. The DC-DC boost converter is chosen, which has a maximum power of 0.5MW. It can be seen in Figure 9, the output voltage closely approaches the value 1kV. Besides, the initial transient state lasts for 2 seconds and then changes to a steady-state rapidly.

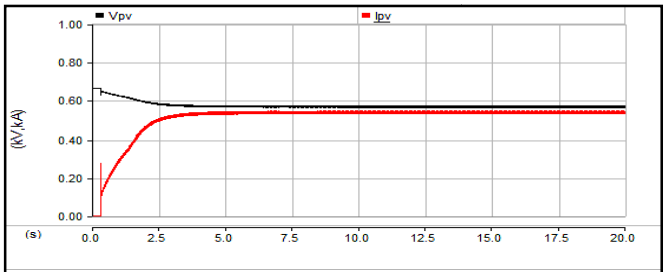

Figure 8. The output voltage and current of array

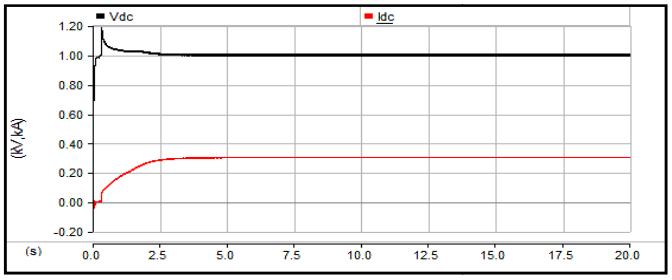

Figure 9. Output voltage and current of the DC-DC boost converter

The simulation is divided into 2 cases study. The first case study, the reactive power generates into the grid is 0.1MVAr, the parameters such as temperature and irradiance are kept constant at 25°C and 1000W/m^2, respectively. All the results about reactive and active power, output three-phase AC voltage, and AC current of the grid-connected inverter are shown in Figures 10, 11, and 12.

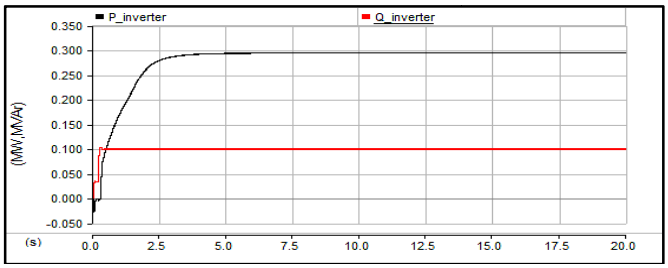

Figure 10. The active and reactive power in case study 1

As can be seen in Figure 10, the starting time until a steady-state is about 5 seconds. P and Q are then maintained at a stable supply to the grid according to the reference values precisely. The transient state occurs in a short time, and there are no fluctuations in the waveform of the voltage and current values. The controlling of reactive power is operated stably, and according to expectation, the implementation of this control model is generally workable. Although there is a loss of active power, this value is small and acceptable.

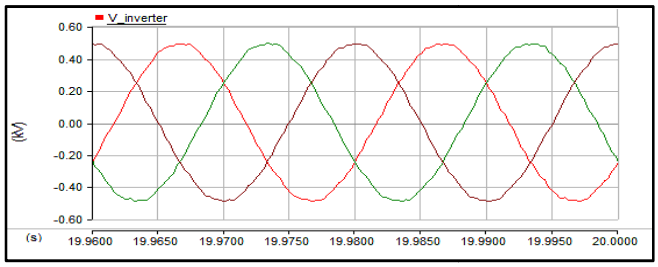

Figure 11. The output voltage of inverter in case study 1

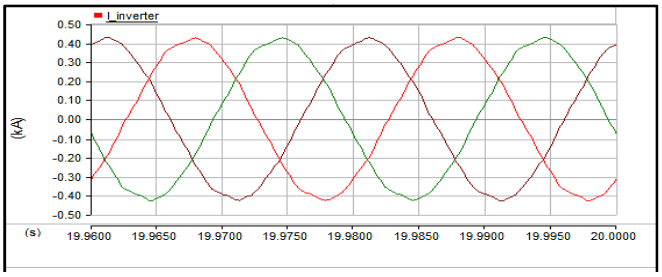

Figure 12. The output current of inverter in case study 1

Figures 11 and 12 show that the waveforms of the output AC voltage and AC current is in stable status. However, the waveforms of output current are distorted because the inverter uses semiconductor components.

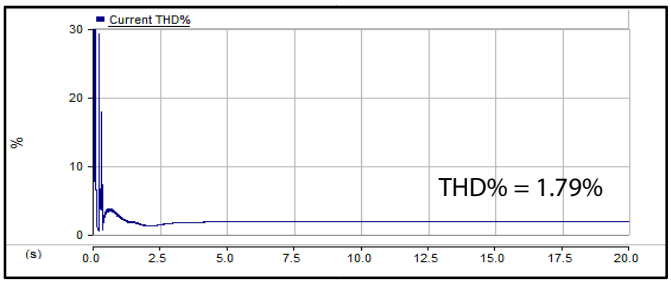

Figure 13. The output current Total Harmonic Distortion in case study 1

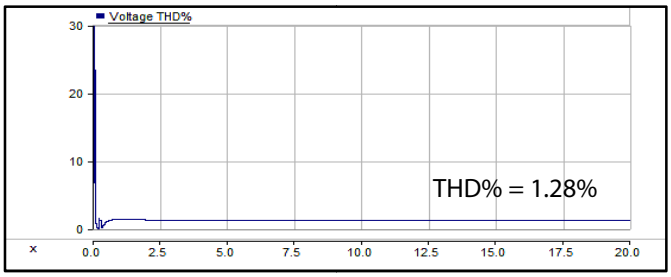

Figure 14. The output voltage Total Harmonic Distortion in case study 1

Figure 13 and Figure 14 show the output current and the output voltage Total Harmonic Distortion (THD), respectively. The current THD% is calculated by simulation is 1.79% that compliant with the Vietnam standard, which requires the current THD%<3%. Besides, the voltage THD% is 1.28%<5% also compliant with the Vietnam standard. The improvement in harmonics, as well as power loss, should be carried out in the next studies through the design of LC filters for systems and technological development to increase the efficiency of the semiconductor valves.

The second case study is focused on the ability to control the reactive power of the system when changes in temperature and radiation occur or due to dispatch commands. During shading conditions, the irradiance sharply decreases. The extent of reduction depends on the type of shading [14]. This problem causes an effect on the performance of the PV system output power. Figure 15 shows the active power and reactive power generated into the grid when the irradiance changes from 1000W/m^2 to 800W/m^2. Whereas, Figure 16 shows the change from 1000W/m^2 to 0W/m^2. The decrease rate is 100W/s.m^2. The reactive power is 0.1MVar.

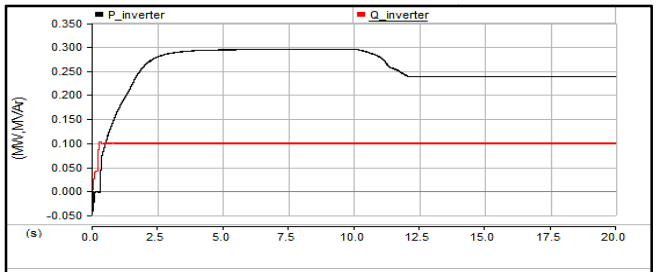

Figure 15. The active and reactive power when the irradiance changes from 1000W/m^2 to 800W/m^2

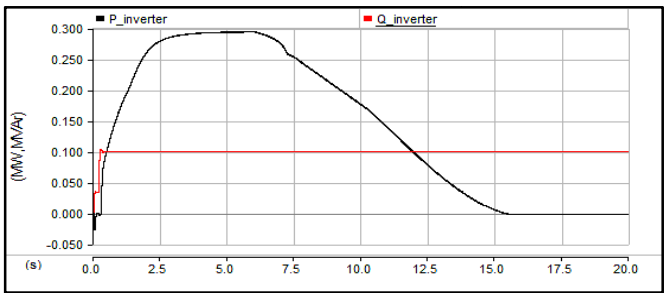

Figure 16. The active and reactive power when the irradiance changes from 1000W/m^2 to 200W/m^2

It can be seen in Figure 15, when the irradiance fell abruptly from 1000W/m^2 to 800W/m^2 at the 10th second, the active power also decreased and stabilized after about 2 seconds at approximately 0.24MW. In Figure 16, the active power decreased to zero in 10 seconds.

During both incidents, the reactive power remained at 1MVAr supply to the grid since reactive power and active power are controlled independently by the Clarke and Park transforms. Thus, the system still operated stably and correctly when environmental conditions changed.

Furthermore, Figure 17 illustrates the possibility of increasing and decreasing the reactive power generated to the grid in case of receiving the dispatch command from the load dispatch centers. In the beginning, the Q is set to 0.1MVAr then abruptly changed from 0.1MVAr to 0.15MVAr at 6th second, finally decreased to 0MVAr at 14th second.

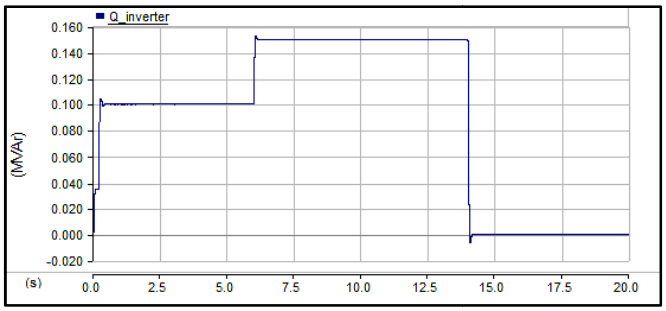

Figure 17. The reactive power of inverter when the reference value is changed

With this *dq*-controller, the system's ability to control reactive power can operate immediately and accurately. Thus it is possible to control the system to keep the power factor at a fixed level. However, the fluctuations in the transient state can be reduced, so the control methods need to be improved in the next studies.

4. CONCLUSIONS

In this paper, a simplified model of a grid-connected PV solar system in PSCAD/EMTDC has been presented with the mathematical formulations. The DC-DC converter is used to increased the input DC side voltage of the inverter. The inverter controls both active and reactive power into the grid. The P&O MPPT algorithms and Park&Clarke transformation and three-phase PLL are described in detail. The simulation results have validated the control method. In the coming studies, improving the voltage and current harmonics of output signals of the inverter will be focused.

REFERENCES

[1]. S. A. Rahman, R. K. Varma, 2011. *PSCAD/EMTDC model of a 3-phase grid connected photovoltaic solar system.*NAPS 2011 - 43rd North Am. Power Symp.

[2]. M. F. Schonardie, D. C. Martins, 2008. *Application of the dq0 transformation in the three-phase grid-connected PV systems with active and reactive power control*. 2008 IEEE Int. Conf. Sustain. Energy Technol. ICSET 2008, pp. 18–23.

[3]. A. Cagnano, E. De Tuglie, M. Liserre, R. A. Mastromauro, 2011. *Online optimal reactive power control strategy of PV inverters.* IEEE Trans. Ind. Electron., vol. 58, no. 10, pp. 4549–4558.

[4]. S. Khadidja, M. Mountassar, B. M'Hamed, 2017. *Comparative study of incremental conductance and perturb & observe MPPT methods for photovoltaic system*. Int. Conf. Green Energy Convers. Syst. GECS 2017.

[5]. H. G. Vu, H. Yahoui, T. Chorot, H. Hammouri, 2012. *Control active and reactive power of Voltage Source Inverter (VSI).* 2nd Int. Symp. Environ. Friendly Energies Appl. EFEA 2012, pp. 308–311.

[6]. A. Cabrera-Tobar, E. Bullich-Massagué, M. Aragüés-Peñalba, O. Gomis-Bellmunt, 2019. *Active and reactive power control of a PV generator for grid code compliance*. Energies, vol. 12, no. 20.

[7]. H. Park, H. Kim, 2013. *PV cell modeling on single-diode equivalent circuit*. IECON Proc. Industrial Electron. Conf., no. 8, pp. 1845–1849.

[8]. H. Bellia, R. Youcef, M. Fatima, 2014. *A detailed modeling of photovoltaic module using MATLAB.* NRIAG J. Astron. Geophys., vol. 3, no. 1, pp. 53–61.

[9]. K. Chatterjee, B. G. Fernandes, G. K. Dubey, 1999. *An instantaneous reactive volt-ampere compensator and harmonic suppressor system.* IEEE Trans. Power Electron., vol. 14, no. 2, pp. 381–392.

[10]. T. Selmi, M. Abdul-Niby, L. Devis, A. Davis, 2014. *P&O MPPT implementation using MATLAB/Simulink.* 2014 9th Int. Conf. Ecol. Veh. Renew. Energies, EVER 2014.

[11]. C. J. O'Rourke, M. M. Qasim, M. R. Overlin, J. L. Kirtley, 2019. *A Geometric Interpretation of Reference Frames and Transformations: dq0, Clarke and Park.* IEEE Trans. Energy Convers., vol. PP, no. c, pp. 1–1.

[12]. E. Muljadi, M. Singh, V. Gevorgian, 2013. *PSCAD Modules Representing PV Generator.* National Renewable Energy Laboratory (NREL).

[13]. B. Liu, F. Zhuo, Y. Zhu, H. Yi, F. Wang, 2015. *A three-phase PLL algorithm based on signal reforming under distorted grid conditions.* IEEE Trans. Power Electron., vol. 30, no. 9, pp. 5272–5283.

[14]. G. Sai Krishna, T. Moger, 2019. *Reconfiguration strategies for reducing partial shading effects in photovoltaic arrays: State of the art.* Sol. Energy, vol. 182, no. February, pp. 429–452.

THÔNG TIN TÁC GIẢ

Nguyễn Quang Thuấn[1], Nguyễn Đức Tuyên[2], Đỗ Văn Long[2], Ninh Văn Nam[1]

[1]Trường Đại học Công nghiệp Hà Nội

[2]Viện Điện, Trường Đại học Bách khoa Hà Nội